Supporting Information

Copper ferrite Nanoparticles loaded on Reduced Graphene Oxide Nanozymes for the Ultrasensitive Colorimetric Assay of Chromium ions

Wenwen Yi, [a] **Peng Zhang,**[a] **Yunpeng Wang,**[a] **Zhongping Li, ***[a,b] **Yujing Guo, ***[a,b] **Meng Liu,** [c] **Chuan Dong,** [a,b] **Changfeng Li***[d]

[a]*Institute of Environmental Science, Shanxi University, Taiyuan 030006, P.R. China.*
[b] *Shanxi Laboratory for Yellow River, Taiyuan 030006, China.*
[c] *School of Environmental Science and Technology, Key Laboratory of Industrial Ecology and Environmental Engineering (Ministry of Education), Dalian University of Technology, Dalian 116024, China.*
[d]*Department of Pharmacy, Changzhi Medical College, Changzhi 046000, Shanxi, P.R. China.*

**Corresponding author :* Zhongping Li, Yujing Guo,Changfeng Li

Email address: zl104@sxu.edu.cn

guoyj@sxu.edu.cn

licf1968@qq.com

1. Reagents and apparatus

Ferric nitrate ($Fe(NO_3)_3$), copper nitrate ($Cu(NO_3)_2 \cdot 3H_2O$), Chromic Chloride hexahydrate ($CrCl_3 \cdot 6H_2O$), sodium hydroxide (NaOH), potassium permanganate ($KMnO_4$) were procured from Aladdin Reagent Co.,Ltd (Shanghai, China). $NaNO_3$, hydrogen peroxide (30% H_2O_2), Sulfuric acid (H_2SO_4, 98%), 3,3′,5,5′-tetramethylbenzidine (TMB) were supplied from Macklin Biochemical Co., Ltd (Shanghai, China). Graphite powder was procured from Tianjin Reagent Factory. All reagents used in this research are analytically grade. Ultrapure water (18.2 MΩ) was used throughout the whole experiments. The working buffer was 0.2 M HAc-NaAc buffer with various pH in the present study.

The morphology of $CuFe_2O_4$/rGO nanozyme was recorded by TEM (JEM-2100 (JEOL, Japan)). The Fourier transform infrared (FT-IR) spectra were obtained on TENSOR II infrared spectrometer (Bruker Germany). X-ray photoelectron spectroscopy (XPS) of $CuFe_2O_4$/rGO was obtained on a Thermo Scientific, ESCALAB 250Xi with Al Kα radiation (USA). UV-vis spectra were carried out on a Perkin Elmer, Lambda 950 UV-vis spectrophotometer.

2. Results and discussion

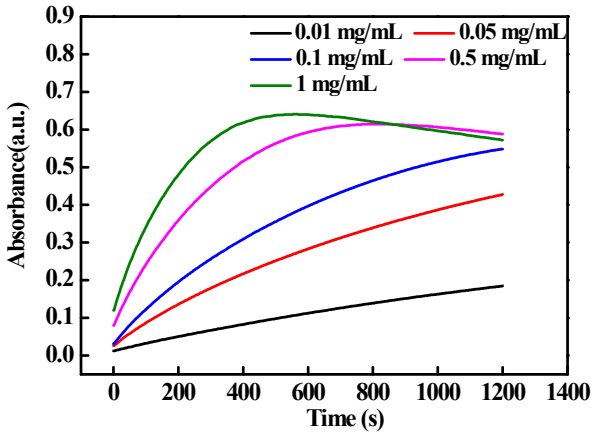

Fig. S1 Time dependent absorbance evolution at 652 nm of TMB with different concentrations of $CuFe_2O_4$/rGO.

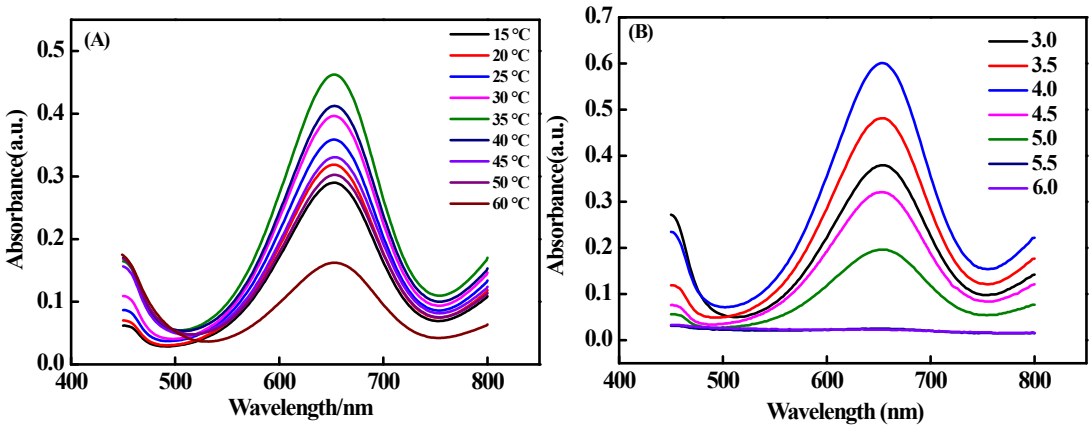

Fig. S2 UV–vis absorbance spectra of the reaction system at 652 nm at different reaction temperatures (A) and pH (B).

$$\frac{1}{\nu} = \frac{K_m}{V_m}\left(\frac{1}{[S]} + \frac{1}{K_m}\right)$$

(eq S1)[1]

where ν is the rate of conversion, V_m the maximum rate of conversion, [S] the substrate concentration, and K_m the Michaelis−Menten constant, which is equivalent to the substrate concentration, since the rate of conversion is half of V_m.

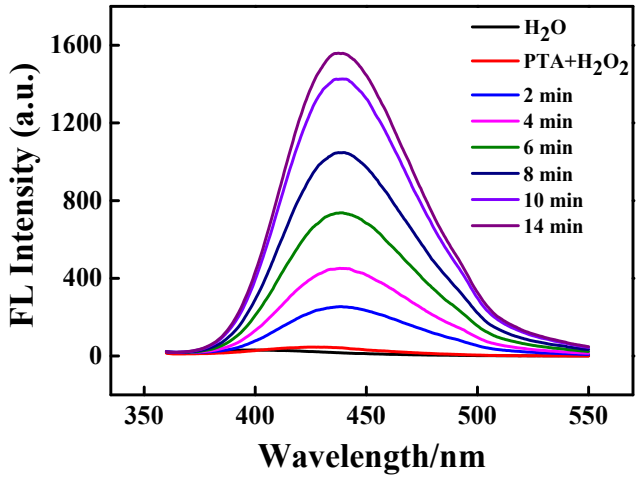

Fig. S3 The fluorescence intensity of the H_2O_2+ $CuFe_2O_4$/rGO systems generated hydroxyl radicals captured by PTA changes with time.

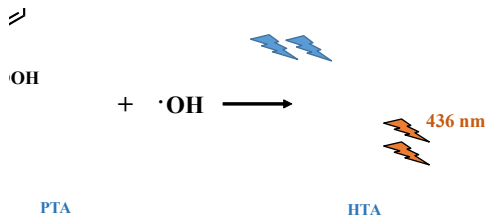

Scheme S2 PTA is combined with hydroxyl radicals to form 2-hydroxy phenylene terephthalic acid.

Due to $CuFe_2O_4$/rGO can be used as a mimetic enzyme, it is obviously an important work to explore its internal catalytic mechanism. Then, we explore the possible peroxidase-like catalytic mechanism of $CuFe_2O_4$/rGO by fluorescence method. Simply, the formation of hydroxyl radicals during the reaction of H_2O_2 catalyzed by $CuFe_2O_4$/rGO was verified by using a p-phthalic acid (PTA) as a fluorescence probe [2]. Non-fluorescent PTA is very easy to bind to hydroxyl radicals to form 2-hydroxy terephthalic acid (HTA) having high fluorescent, which typically emits unique blue fluorescence near 436 nm by excitation at 315 nm [3] (see in scheme S2). In Fig. S3 indicates the fluorescence intensity of H_2O, PTA-H_2O_2 and PTA-H_2O_2 -catalyst with time. As can be seen, no fluorescence emission was observed without the catalyst. However, in the presence of catalyst, the fluorescence intensity revealed a significant increase with increasing time, confirming that·OH is derived from the decomposition of H_2O_2 by the catalysis of $CuFe_2O_4$/rGO nanozyme and resulted in the oxidation of PTA to form HTA. This result indicates that the $CuFe_2O_4$/rGO has high catalytic activity with other materials having a consistent like-peroxidase properties.

At the same time, reactive oxygen species (·OH, $O_2^{\cdot-}$, etc.) that may be generated by $CuFe_2O_4$/rGO in the catalytic H_2O_2 reaction can be proved by radical inhibition experiments. The introduction of TBA as a scavenging agent of ·OH can be seen from Figure S4 (A), with the addition of TBA, the absorbance of the solution decreased significantly, further proving the existence of ·OH in the system [4,5]. PBQ was taken as the scavenging agent of $O_2^{\cdot-}$, as shown in Figure S4 (B), the absorbance of the solution did not change significantly, indicating the $O_2^{\cdot-}$ was almost not produced during the catalytic oxidation process [6]. To further confirm the generation of ·OH in the catalytic system, EPR analysis was performed with 5,5- dimethyl-1-pyrroline N-oxide (DMPO),

as presented in Figure S5. In DMPO trapping spectra of the EPR tests, the intensified peaks of DMPO-HO· could be identified, indicating the existence of ·OH radicals [7].

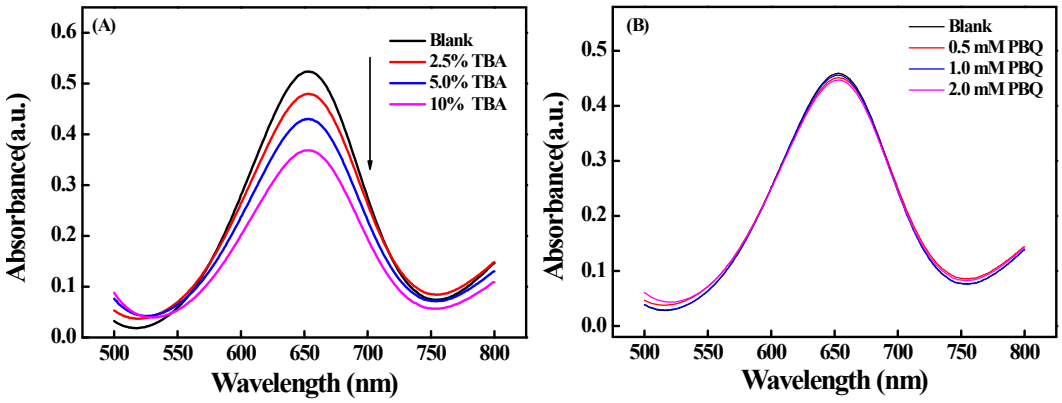

Fig. S4 Absorbance changes of TMB+H_2O_2+$CuFe_2O_4$/rGO system after addition of different concentrations of TBA and PBQ.

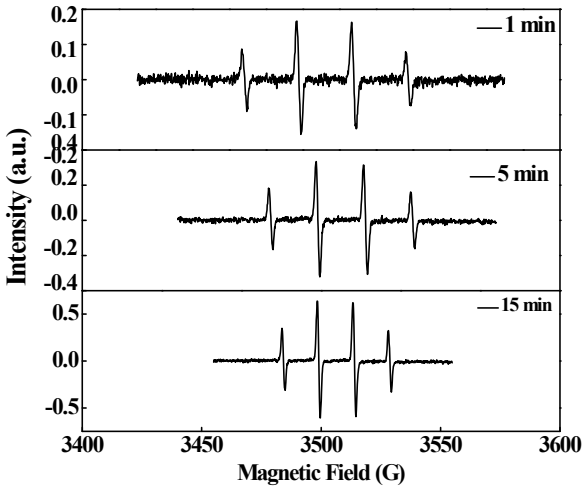

Fig. S5 EPR spectra in H_2O_2+$CuFe_2O_4$/rGO system with DMPO as the trapping agent.

Table S1. Comparison of kinetic parameters for the oxidation of TMB by different nanomaterials

Catalyst	K_m [mM]		V_m[$10^{-8}Ms^{-1}$]		References
	H_2O_2	TMB	H_2O_2	TMB	
HRP	3.70	0.434	8.71	10.0	[8]
Au/HZIF-8@TCPP(Fe)	1.74	0.79	9.60	7.26	[9]
Cu-MOF	6.41	4.11	10.21	55.56	[10]
Cu-Ag/rGO	8.6245	0.6340	4.2553	7.0175	[11]
Au-NCs+ ZIF-8/CQDs	16.86	13.29	1.429	2.941	[12]
MoS_2-Fe_3O_4	2.50	0.35	3.3	35	[13]
$CoFe_2O_4$	8.89	0.387	1.93	2.90	[14]
Graphene nanoribbons	3.52	0.42	3.09	1.58	[15]
$CuFe_2O_4$/rGO	0.453	0.47	1.778	65.1	this work

Table S2 Comparison of differently colorimetric methods for determination of Cr^{3+}

Materials	Linear range(μM)	LOD(nM)	Ref.
TADA@AuNPs	0.5-5	5.89	[16]
silver nanoflakes	-	1.4/11.5	[17]
gold nanoparticles	12.5-75	1.15×10^4	[18]
Silver nanopentagons	80-10000	5×10^4	[19]
4-MBA–AuNPs	20-25	5000	[20]
Citrate- and thiourea-AuNPs	-	500	[21]
PMAA@Au NPs	-	4×10^4	[22]
NiCNF-RhB	-	203	[23]
AuNBP@Ag NRs	0.01-100	8.7	[24]
N-T/AuNPs	0.5-2.5	30	[25]
MUA-AuNPs	0.0001-1	0.017	[26]
CTP- AgNPs	18.75-62.5	6.25×10^3	[27]
$CuFe_2O_4$/rGO	0.1-25	35	This work

References

[1] J. L. Zhu, X. Peng, W. Nie, Y. J. Wang, J. W. Gao, W. Wen, J. N. Selvaraj, X. H. Zhang and S. F. Wang, Hollow copper sulfide nanocubes as multifunctional nanozymes for colorimetric detection of dopamine and electrochemical detection of glucose, Biosens. Bioelectron., 2019, **141**, 111450.

[2] L. L. Zhou, Q. Guan, Y. A. Li, Y. Zhou, Y. B. Xin and Y. B. Dong, One-Pot Synthetic Approach toward Porphyrinatozinc and Heavy-Atom Involved Zr-NMOF and Its Application in Photodynamic Therapy, Inorg. Chem., 2018, **57**, 3169-3176.

[3] M. Amirzehni, J. Hassanzadeh and B. Vahid, Surface imprinted CoZn-bimetalic MOFs as selective colorimetric probe: application for detection of dimethoate, Sensor. Actuator. B Chem., 2020, **325**, 128768.

[4] P. J. Ni, Y. J. Sun, H. C. Dai, J. T. Hu, S. Jiang, Y. L. Wang and Z. Li, Highly sensitive and selective colorimetric detection of glutathione based on Ag [I] ion-3,3 ',5,5 '-tetramethylbenzidine (TMB), Biosens. Bioelectron., 2015, **63**, 47-52.

[5] D. Bano, V. Kumar, V. K. Singh, S. Chandra, D. K. Singh, P. K. Yadav, M. Talat and S. H. Hasan, A facile and simple strategy for the synthesis of label free carbon quantum dots from the latex of euphorbia milii and its peroxidase-mimic activity for the naked eye detection of glutathione in a human blood serum, ACS Sustain. Chem. Eng., 2019, **7**, 1923-1932.

[6] C. X. Chen, D. Zhao, Y.Y. Jiang, P. J. Ni, C. H. Zhang, B. Wang, F. Yang, Y. Z. Lu and J. Sun, Logically regulating peroxidase-like activity of gold nanoclusters for sensing phosphate-containing metabolites and alkaline phosphatase activity, Anal. Chem., 2019, **91**, 15017-15024.

[7] X. J. Zheng, Q. Zhu, H. Q. Song, X. R. Zhao, T. Yi, H. L. Chen and X. G. Chen, In situ synthesis of self-assembled three-dimensional graphene-magnetic palladium nanohybrids with dual-enzyme activity through one-pot strategy and its application in glucose probe, ACS Appl. Mater. Interfaces, 2015, **7**, 3480-3491.

[8] L. Gao, J. Zhuang, L. Nie, J. Zhang, Y. Zhang, N. Gu, T. Wang, J. Feng, D. Yang, S. Perrett and X. Yan, Intrinsic peroxidase-like activity of ferromagnetic nanoparticles, Nat. Nanotechnol., 2007, **2**, 577-583.

[9] H. Z. Zhang, H. Y. Wu, X. G. Qin, Y. Shen, X. L. Wei and G. Liu, Metalloporphyrin and gold nanoparticles modified hollow zeolite imidazole Framework-8 with excellent peroxidase like activity for quick colorimetric determination of choline in infant formula milk powde,Food Chem., 2022, **384**, 132552.

[10] C. Wang, J. Gao and H. Tan, Integrated antibody with catalytic metal-organic framework for colorimetric immunoassay, ACS Appl. Mater. Inter., 2018, **10**, 25113-25120.

[11] G. Darabdhara, B. Sharma, M. R. Das, R. Boukherroub and S. Szunerits, Cu-Ag bimetallic nano- particles on reduced graphene oxide nanosheets as peroxidase mimic for glucose and ascorbic acid detection, Sens. Actuators B: Chem., 2017, **238**, 842-851.

[12] F. P. Ran, Y. X. Xu, M. R. Ma, X. Y. Liu and H. X. Zhang, Flower-like ZIF-8 enhance the peroxidase-like activity of nanoenzymes at neutral pH for detection of heparin and protamine, Talanta, 2022, 250, 123702.

[13] J. Liu, J. Du, Y. Su and H. Zhao, A facile solvothermal synthesis of 3D magnetic MoS_2/Fe_3O_4 nanocomposites with enhanced peroxidase-mimicking activity and colorimetric detection of perfluorooctane sulfonate, Microchem. J, 2019, **149**, 104019.

[14] L. Wu, G. Wan, N. Hu, Z. He, S. Shi, Y. Suo, K. Wang, X. Xu, Y. Tang and G. Wang, Synthesis of Porous $CoFe_2O_4$ and Its Application as a Peroxidase Mimetic for Colorimetric Detection of H_2O_2 and Organic Pollutant Degradation, Nanomaterials, 2018, **8**, 451.

[15] S. Rostami, A. Mehdinia and A. Jabbari, Intrinsic peroxidase-like activity of graphene nanoribbons for label-free colorimetric detection of dopamine, C Mater. Sci. Eng. C, 2020, **114**, 111034.

[16] P. Mondal and J. L. Yarger, Colorimetric Dual Sensors of Metal Ions Based on 1,2,3-Triazole-4,5-Dicarboxylic Acid-Functionalized Gold Nanoparticles, J. Phys. Chem. C, 2019, **123**, 20459-20467.

[17] X. M. Li, S. T. Zhang, Y. F. Dang, Z. Y. Liu, Z. Zhang, D. L. Shan, X. H. Zhang, T. S. Wang and X. Q. Lu, Ultratrace Naked-Eye Colorimetric Ratio Assay of Chromium(III) Ion in Aqueous Solution via Stimuli-Responsive Morphological Transformation of Silver Nanoflakes, Anal. Chem., 2019, **91**, 4031-4038.

[18] S. Bothra, R. Kumar and S. K. Sahoo, Pyridoxal conjugated gold nanoparticles for distinct colorimetric detection of chromium(III) and iodide ions in biological and environmental fluids, New J. Chem., 2017, **41**, 7339-7346.

[19] Z. K. Zhang, D. A. Guo, C. X. Hu and Y. M. Liu, Silver nanopentagons-based colorimetric sensor for high-selective chromium(III) detection in aqueous solution with polyvinylpyrrolidone and citrate, Chem. Pap., 2021, **75**, 5535-5541.

[20] Z. K. Zhang, X. J. Ye, Q. Q. Liu, Y. M. Liu, and R. J. Liu, Colorimetric detection of Cr^{3+} based on gold nanoparticles functionalized with 4-mercaptobenzoic acid, J Anal. Sci. Technol., 2020, **11**.

[21] D. Y. Long, and H. L. Yu, A synergistic coordination strategy for colorimetric sensing of chromium(III) ions using gold nanoparticles, Anal. Bioanal. Chem., 2016, **408**, 8551-8557.

[22] J. B. Li, C. Han, W. L. Wu, S. J. Zhang, J. W. Guo and H. Y. Zhou, Selective and cyclic detection of Cr^{3+} using poly (methylacrylic acid) monolayer protected gold nanoparticles, New J Chem., 2014, **38**, 717-22.

[23] D. Kumar and N. Talreja, Nickel nanoparticles-doped rhodamine grafted carbon nanofibers as colorimetric probe: Naked eye detection and highly sensitive measurement of aqueous Cr^{3+} and Pb^{2+}, Korean J. Chem. Eng., 2019, **36**, 126-135.

[24] X. Q. Song, X. Chen, Z. X. Liang, D. Xu and Y. Liang, A colorimetric sensing probe for chromium (III) ion based on domino like reaction, Colloid. Surface. B, 2022, **215**, 112494.

[25] J. J. Du, H. Y. Ge, Q. Y. Gu, H. Du, J. L. Fan and X. J. Peng, Gold nanoparticle-based nano-probe for the colorimetric sensing of Cr^{3+} and $Cr_2O_7^{2-}$ by the coordination strategy, Nanoscale, 2017, **9**, 19139-19144.

[26] R. Q. Zhu, J. P. Song, Y. Zhou, P. Lei, Z. P. Li, H. W. Li, S. M. Shuang and C. Dong, Dual sensing reporter system of assembled gold nanoparticles toward the sequential colorimetric detection of adenosine and Cr(III), Talanta, 2019, **204**, 294-303.

[27] L. Zhan, T. Yang, S. J. Zhen and C. Z. Huang, Cytosine triphosphate-capped silver nanoparticles as a platform for visual and colorimetric determination of mercury(II) and chromium(III), Microchim. Acta, 2017, **184**, 3171-3178.